Elastic wave propagation along waveguides in three-dimensional phononic crystals

H. Chandra,[1] P. A. Deymier,[1] and J. O. Vasseur[2]
[1]*Department of Materials Science and Engineering, University of Arizona, Tucson, Arizona 85721, USA*
[2]*Laboratoire de Dynamique et Structure des Matériaux Moléculaires, UMR CNRS 8024, Université de Lille1, 59655 Villeneuve d'Ascq Cedex, France*
(Received 22 January 2004; published 26 August 2004)

We investigate theoretically using the finite difference time domain method acoustic wave propagation along waveguides in three-dimensional phononic crystals constituted of lead spherical inclusions on a face-centered cubic lattice embedded in an epoxy matrix. The transmission spectra of the perfect phononic crystal for transverse and longitudinal acoustic waves are shown to depend strongly on the direction of propagation. The crystal possesses an absolute band gap. Waveguides oriented along different crystallographic directions, namely the ⟨100⟩ and ⟨111⟩ directions, exhibit pass bands in the phononic crystal band gaps for both transverse and longitudinal polarizations.

DOI: 10.1103/PhysRevB.70.054302 PACS number(s): 63.20.−e, 43.20.+g, 43.40.+s

I. INTRODUCTION

Acoustic band gap materials (ABG), also known as phononic crystals, are inhomogeneous media constituted of two- or three-dimensional periodic arrays of inclusions embedded in a matrix. A large contrast between the elastic parameters and the mass density of the inclusions and of the matrix is a necessary condition for the existence of band gaps in the acoustic band structure of these composite materials.[1] Theoretical studies have demonstrated the existence of absolute band gaps[2–4] prior to their experimental observation in various two-dimensional (2D) phononic crystals constituted of solid components[5,6] or mixed solid/fluid components.[7–9] Recent investigations of perfect and defected phononic crystals have revealed a rich range of behaviors, such as those associated with (a) linear and point defects,[10] (b) wave bending and splitting,[11] and (c) transmission through perfect[12,13] or defect-containing[13] waveguides. Waveguides in 2D phononic crystals are produced, for instance, by removing cylindrical inclusions along one or several rows of the inclusion array. The insertion of defects, such as resonant cavities, inside or at the edge of a waveguide[13] was shown to give rise to the filtering or to the rejection of selective frequencies in the guide's transmission spectrum.

Theoretical and experimental studies of elastic wave propagation in three-dimensional (3D) phononic crystals have revealed the existence of full band gaps in two-component face-centered cubic (fcc) lattices of mercury spheres in aluminum matrix,[14] lead spheres in epoxy,[15] tungsten carbide in water,[16] steel in polyester,[17] silica in ice,[18] three-component composites of coated spheres in a matrix,[19,20] and hexagonal close packed (hcp) structure of steel spheres in water.[21] Psarobas *et al.* have also studied 3D phononic crystals containing planar defects in the form of, for instance, a plane of impurity spheres.[22] To our knowledge, no work on elastic wave propagation along waveguides in 3D phononic crystals has been reported. The objective of the present publication is to fill in this void and initiate a computer simulation based on theoretical study of acoustic wave propagation in 3D phononic crystals containing linear waveguides. Similarly to their 2D counterparts, waveguides in 3D phononic crystals are constructed by removing a row of inclusions (e.g., spheres) along some particular crystallographic direction of the crystal lattice. We focus on simple linear waveguides which provide a basis for developing more complicated structures such as bent waveguides, defected waveguides with filtering resonances, and mixed waveguides.[23]

The calculations performed in this work are based on the finite difference time domain (FDTD) method that has been proven to be an efficient method for obtaining both the transmission coefficient[5,15,24] and the dispersion curves[25,26] in phononic crystals.

The organization of the paper is as follow. The models and the method of calculation are briefly presented in Sec. II. The FDTD results of propagation along waveguides in 3D phononic crystals are reported and discussed in Sec. III. Some conclusions concerning the transmission along more complex 3D waveguides are given in Sec. IV.

II. METHOD OF CALCULATION AND MODELS

The FDTD method has been used extensively with success to simulate the propagation of electromagnetic waves in photonic band gap materials.[27–29] In recent years, the FDTD method has been extended to simulating elastic wave propagation in phononic crystals.[5,15,24] This method solves the elastic wave equation by discretizing time and space and by replacing derivatives by finite differences. We employ a spatial grid with mesh size $\Delta x=\Delta y=\Delta z=0.2$ mm. The time integration step, Δt, is 10.2 ns. The total number of 1.2 ns time steps used in our calculations is time steps for a total of 1.3×10^{-3} s. The wave equation is solved using second-order centered finite-difference expressions for the space and time derivatives.

Here, we use the FDTD method to calculate the transmission coefficient of finite thickness samples of 3D phononic crystals. For this, the model systems are composed of three parts along the direction of propagation, *Y*. The central region contains the finite size inhomogeneous phononic composite. This region is sandwiched between two homogeneous media, 1 cm long, used for launching and probing the acoustic waves. Absorbing Mur boundary conditions[30] are applied

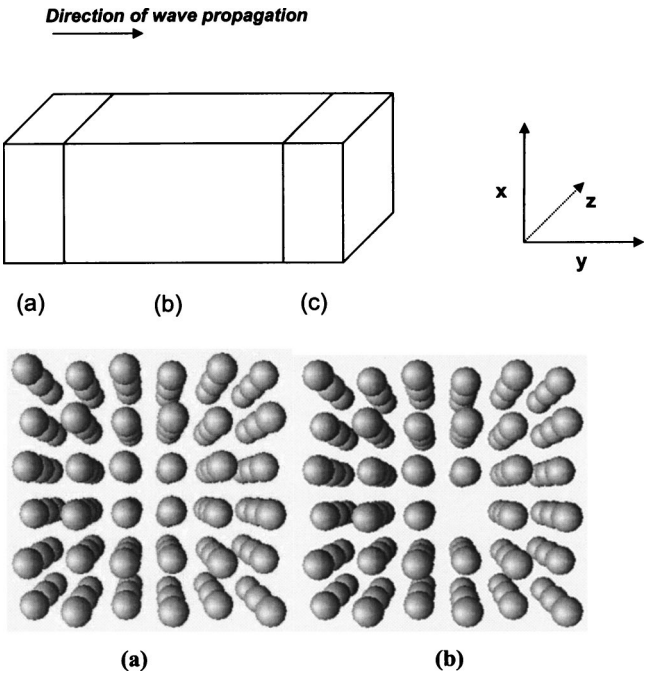

FIG. 1. (Top) The overall model used for calculation. (a) and (c) are the homogeneous regions and (b) is the inhomogeneous region containing the phononic crystal. (bottom) (a) 3D phononic crystals composed of spherical inclusions on a fcc lattice shown along the [100] direction and (b) phononic crystal with a linear waveguide along the [100] direction. Both crystals are constituted of 3 fcc unit cells $\times 3$ fcc unit cells $\times 3$ fcc unit cells.

at the free ends of the homogeneous regions to avoid any undesirable reflections.

Our phononic crystal is composed of lead spheres inclusions arranged on a fcc lattice embedded in an epoxy host matrix. This composite system is known to possess absolute gaps in its band structure.[15,31] The lattice constant, a_0, is 6 mm. The packing factor, f, which is defined as $f=\frac{16}{3}\pi r^3/a_0^3$ is set to 29.4%. The radius, r, of these inclusions is $0.26a_0$ or 1.56 mm.

The physical and elastic constants of lead and epoxy used in our calculation are as follow: The density of lead and expoxy are 11357 and 1160 kg/m^3, respectively. The longitudinal, C_l, and transverse, C_t, speeds of sound in lead are 2.158 and 0.86 km/s respectively. In epoxy C_l and C_t are 2.83 and 1.16 km/s, respectively.

The finite phononic crystals with or whitout a waveguide consist of 3 fcc unit cells $\times 3$ fcc unit cells in the X and Z plane while the number of unit cells in the direction of propagation, Y, varies from 4 to 7 cells. Periodic boundary conditions (PBC) are imposed in both the X and Z directions. If a wave propagates out of the system in one of these directions, it will re-enter from the opposite side. The waveguide structures are constructed by removing a row of inclusions from the perfect crystal along some chosen crystallographic direction. The model is illustrated in Fig. 1 for a phononic crystal with and without a waveguide along the $\langle 100\rangle$ crystallographic direction. Note that applying PBC to a simulated system containing a waveguide leads to the creation of 8 additional parallel waveguides in the periodic images.

A broadband probe wave packet is launched in the first homogeneous region of the simulated system.[24] The incoming wave is uniform in the XZ plane and propagates along the Y axis. The displacement has a Gaussian profile along the Y direction. The displacement of the probing signal is nonzero along the Y and X directions for longitudinal and transverse waves, respectively. The Y component of the displacements for longitudinal modes and the X component of the displacement for transverse modes of the transmitted wave are collected at the end of the second homogeneous region. For the perfect phononic crystals, the displacements are averaged over the XZ plane. In the case of systems with waveguides, we average the displacements only over the inner cross section of the guide. These average displacements as a function of time are then Fourier transformed. The transmission coefficient is defined as the ratio of the Fourier transform of the average displacements in the composite to the Fourier transform of the average displacements in a homogeneous matrix medium. Because of the limited area over which the displacement is averaged for phononic crystals

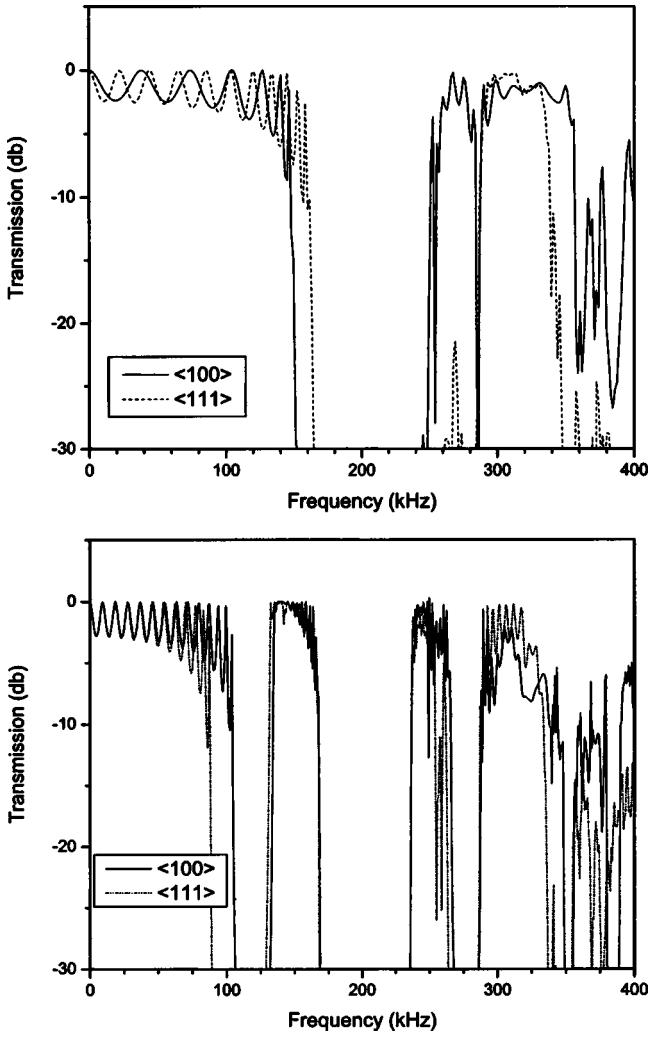

FIG. 2. Calculated elastic wave transmission spectra for a fcc lattice of lead sphere in an epoxy matrix for propagation along the $\langle 100\rangle$ and $\langle 111\rangle$ directions. Top: Longitudinal incident waves. Bottom: Transverse incident waves.

TABLE I. Frequency range for the first and second transmission gaps for longitudinal and transverse elastic waves in 3D lead/epoxy fcc phononic crystal.

	Frequency (kHz)			
Longitudinal	First gap	Second gap	First gap (Ref. 15)	Second gap (Ref. 15)
⟨100⟩	150–248	⋯	153–246	⋯
⟨111⟩	160–262	272–284	⋯	⋯
Transverse				
⟨100⟩	105–134	168–236	120–138	183–244
⟨111⟩	89–128	169–236	⋯	⋯

with a waveguide, the transmission coefficient may exceed one. The transmission coefficients as a function of frequency are reported in decibels.

III. RESULTS AND DISCUSSION

A. Transmission in phononic crystals

In this section we consider the propagation of longitudinal and transverse elastic waves in the lead/epoxy 3D fcc phononic crystal along the ⟨100⟩ and ⟨111⟩ crystallographic directions. Figure 2 shows the transmission spectra in the ⟨100⟩ direction and in the ⟨111⟩ direction for both longitudinal and transverse modes. In the ⟨100⟩ direction and for longitudinal waves, only one gap exists in the interval $[150,248]$ kHz. In contrasts, the transmission spectrum for the ⟨111⟩ direction shows several gaps. The first gap occurs between 160 and 262 kHz. Two other gaps lie in the intervals $[272,284]$ kHz and $[382,406]$ kHz.

The transverse wave transmission spectra show more structure in both ⟨100⟩ and ⟨111⟩ directions compared to the spectra for longitudinal waves in the same directions. There

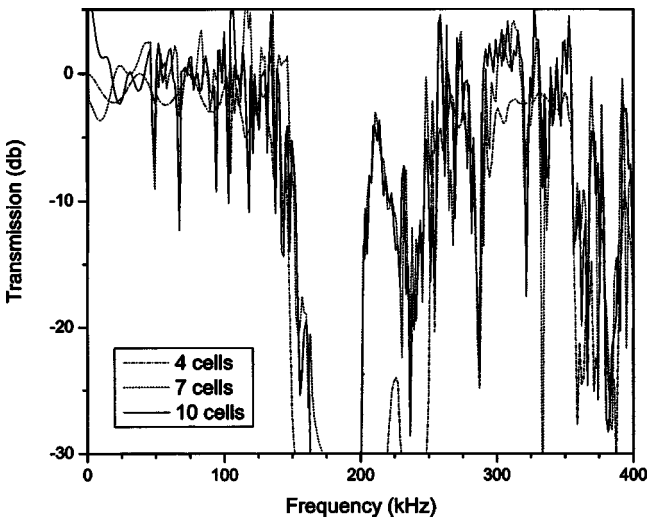

FIG. 3. Effect of guide length on the transmission spectrum of longitudinal waves through a phononic crystal containing a waveguide along the ⟨100⟩ direction.

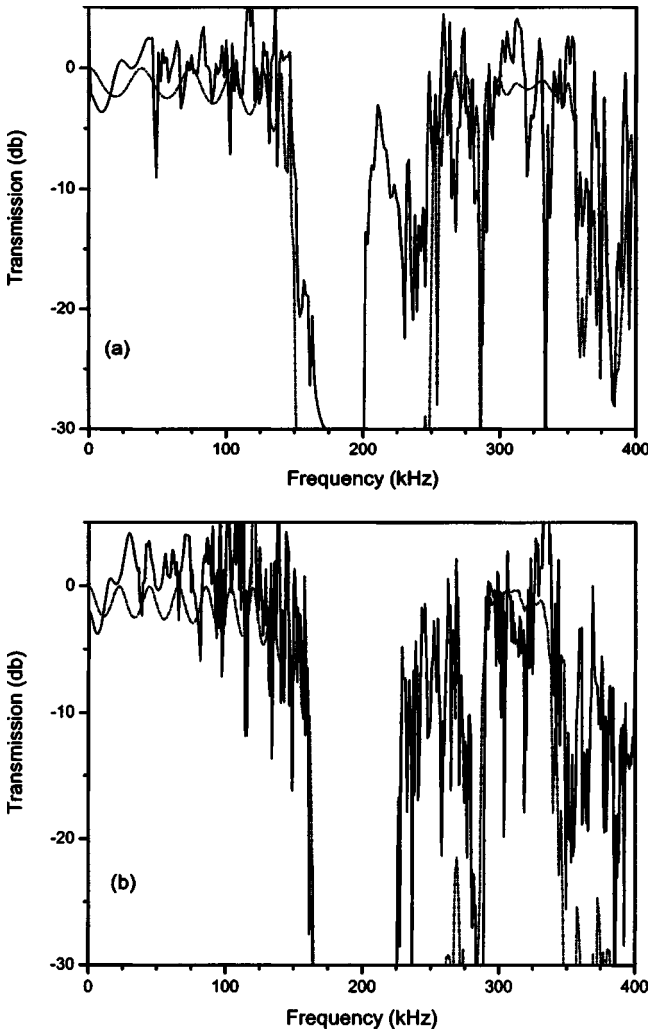

FIG. 4. Transmission spectrum for elastic wave propagation along the (a) ⟨100⟩ direction, and (b) ⟨111⟩ direction. The incident waves are longitudinal. Solid lines represent transmission inside a waveguide while dashed lines refer to transmission of the perfect phononic crystal.

are four gaps in the transverse ⟨100⟩ transmission spectrum. They are located at 105–134 kHz, 168–236 kHz, 266–287 kHz, and 350–360 kHz. There are several gaps in the ⟨111⟩ direction for the propagation of transverse mode. The major gaps in the ⟨111⟩ direction are in the frequency ranges 89–128 kHz, 169–236 kHz, 264–285 kHz, and 341–360 kHz. There are also several additional narrow gaps at higher frequency. As reported in Table I, the ⟨100⟩ results for longitudinal waves are in a good agreement with those reported in the literature for a similar phononic crystal.[15,31] Any deviation in the gap frequencies would be due to the different speeds of sound in epoxy used by different authors. However, there are no published results for transmission spectrum in the ⟨111⟩ direction through the lead-epoxy 3D phononic crystal. Our calculations confirm that an absolute phononic gap does exist in this system. The absolute gap corresponds to the intersection between gaps in different directions. Here, we expect the first full gap to range approximately from 169 to 236 kHz.

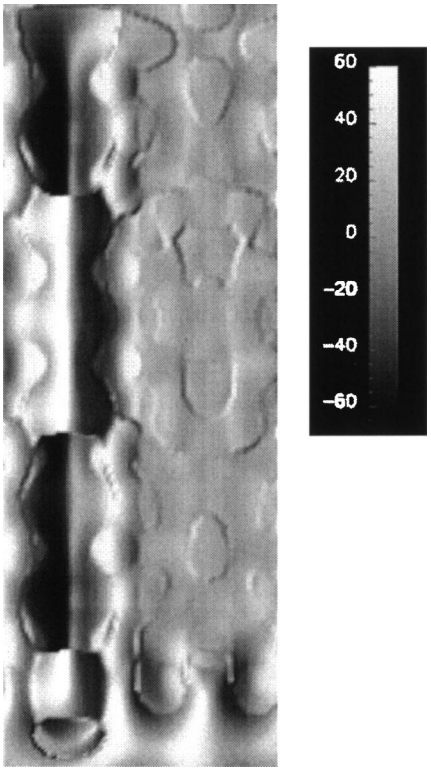

FIG. 5. The square of the field amplitude over a phononic crystal containing a linear ⟨100⟩ waveguide. The incident wave is a longitudinal monochromatic plane wave with requency, $f = 217$ kHz.

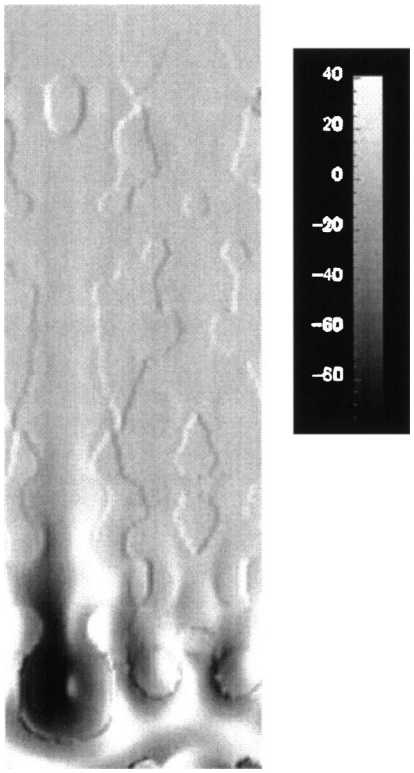

FIG. 6. The square of the field amplitude over a phononic crystal containing a linear ⟨100⟩ waveguide. The incident wave is a longitudinal monochromatic plane wave with frequency, $f = 190$ kHz.

B. Transmission along waveguides in 3D phononic crystals

It has been recognized that the propagation of elastic waves in waveguides formed in phononic crystals depends on the periodic modulation of the elastic constants at the guide boundaries[12] and the calculation of the transmission spectrum is sensitive to the length of the waveguide.[13] We, therefore, conducted an initial series of simulations to examine the optimum waveguide length for convergence of the transmission spectrum. We consider the propagation of longitudinal incident waves along a waveguide in the ⟨100⟩ direction. The model consists of 3 fcc unit cells $\times 3$ unit cells in both the X and Z directions. The length in the direction of propagation, Y, is varied from 4 to 10 unit cells. The transmission spectra are shown in Fig. 3. These calculations clearly show that a four-cell long waveguide is too short for convergence. The spectra for 7 and 10 cells have nearly converged to the same form and intensity. Consequently, we set the length of the system to 7 cells in the Y direction for all subsequent waveguide calculations. This is a satisfactory compromise between accuracy and calculation time.

Figure 4 illustrates the transmission spectrum for incident longitudinal waves in linear ⟨100⟩ and ⟨111⟩ waveguides. The waveguide in ⟨100⟩ direction exhibits a well-defined passing band that falls within the stop band of the perfect phononic crystal. The ⟨100⟩ waveguide passing band extends over the range of frequencies 201–248 kHz with maximum transmittivity near 215 kHz. There is also a weak transmission band between 150–175 kHz at the lower edge of the first stop band of the phononic crystal. The ⟨111⟩ waveguide possesses a broad passing band between 225 and 280 kHz.

The time-averaged square of the Y-component of the displacement field, over a two-dimensional cut throughout the phononic crystal with the linear ⟨100⟩ waveguide, for two incident monochromatic plane waves is reported in Figs. 5 and 6. The frequencies of the incident waves are chosen at 217 and 190 kHz such that the first one lies inside the waveguide's passing band and the latter one below the passing band and inside the phononic crystal stop band. Propagation of the plane wave with the highest frequencies is very clear in Fig. 5, while the incident wave with the lower frequency is rapidly attenuated. In this system because of PBC, the simulated system contains parallel waveguides separated by two unit cells of the fcc phononic crystal. Because of that separation, we expect some leakage between the guides, but also note from Figs. 5 and 6 that leakage appears to be relatively small compared to the amplitude of the incident plane wave.

Finally, Fig. 7 shows the transmission spectra for transverse incident waves in phononic crystals containing ⟨100⟩ and ⟨111⟩ linear waveguides. Both systems show weak transmission throughout the first and third stop bands of the phononic crystal. The ⟨100⟩ waveguide does not transmit for most frequencies located within the second stop band of the perfect crystal but near its upper edge in the range 225–248 kHz. A similar behavior is observed for propaga-

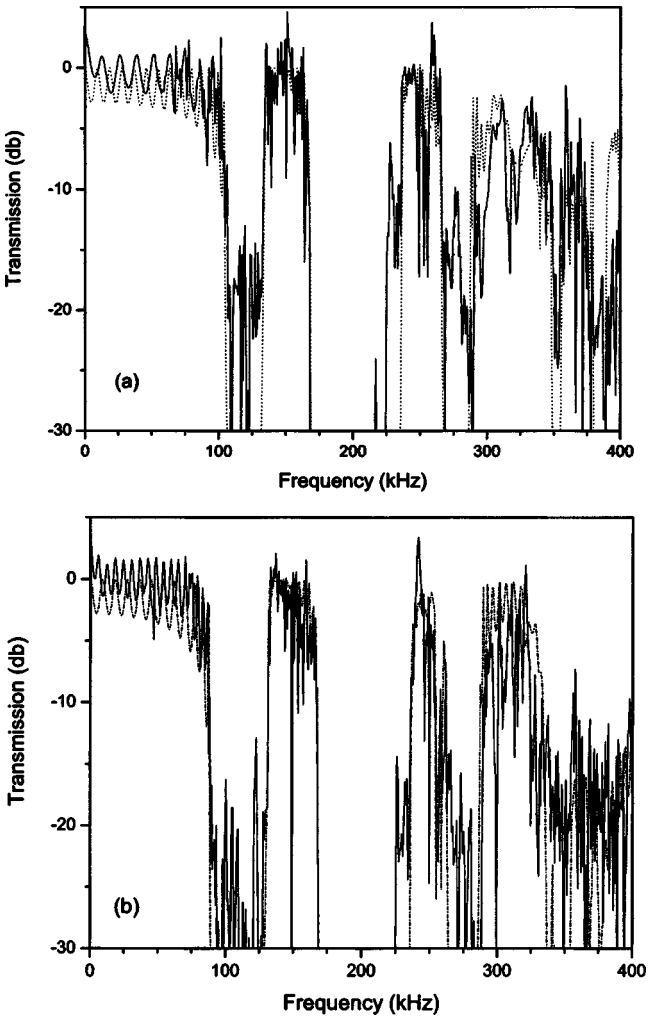

FIG. 7. Transmission spectrum for elastic wave propagation along the (a) ⟨100⟩ direction, and (b) ⟨111⟩ direction. The incident waves have the transverse polarization. Solid lines represent transmission inside a waveguide while dashed lines refer to transmission of the perfect phononic crystal.

tion in the ⟨111⟩ direction, with transmission in the second stop band at frequencies in the interval [224,233] kHz.

IV. CONCLUSIONS

The 3D fcc lead-epoxy phononic crystal exhibits complete elastic gap (i.e., absolute gap) for frequencies between 168 and 236 kHz. Waveguides, formed by removing a row of spherical inclusions along some chosen crystallographic direction of the phononic crystal, exhibit passing bands. The passing bands are in ranges of frequency for which incident waves propagate along the guide but do not propagate in the phononic crystal. Both crystallographic orientations studied here, namely the ⟨100⟩ and ⟨111⟩ directions show passing bands for longitudinal and transverse incident waves in the first stop band of the perfect crystal corresponding to these crystallographic directions. We observe weaker transmission in the case of transverse waves. The longitudinal wave pass band in the ⟨100⟩ and ⟨111⟩ directions do not extend throughout the first stop band but are limited to frequencies near its upper edge. These longitudinal passing bands overlap only partially implying that a bent waveguide with ⟨100⟩ and ⟨111⟩ segments could only transmit longitudinal waves with frequencies corresponding to the intersection between the frequency intervals of the two respective pass bands. The second stop band for transverse waves is only weakly perturbed near its upper edge by the insertion of a waveguide in the phononic crystal.

Finally, in the present paper, we considered only simple linear waveguides formed by removing a row of spherical inclusions of the 3D phononic crystal. As suggested by previous studies of waveguides in 2D phononic crystals,[13,23,26] future work on guidance of elastic wave in 3D phononic crystals will include waveguides constituted of spheres with different diameters or physical properties (impurity spheres), waveguides of hollow spheres in a crystal of filled spheres, as well as waveguides with resonant cavities and/or side branches.

[1] For a review, see M. S. Kushwaha, Recent Res. Devel. Applied Phys. **2**, 743 (1999).
[2] M. S. Kushwaha, P. Halevi, L. Dobrzynski, and B. Djafari-Rouhani, Phys. Rev. Lett. **71**, 2022 (1993); J. O. Vasseur, B. Djafari-Rouhani, L. Dobrzynski, M. S. Kushwaha, and P. Halevi, J. Phys.: Condens. Matter **6**, 8759 (1994).
[3] M. M. Sigalas and E. N. Economou, Solid State Commun. **86**, 141 (1993).
[4] M. S. Kushwaha, Appl. Phys. Lett. **70**, 3218 (1997).
[5] J. O. Vasseur, P. A. Deymier, B. Chenni, B. Djafari-Rouhani, L. Dobrzynski, and D. Prevost, Phys. Rev. Lett. **86**, 3012 (2001).
[6] R. E. Vines, J. P. Wolfe, and A. V. Every, Phys. Rev. B **60**, 11 871 (1999).
[7] F. R. Montero de Espinosa, E. Jimenez, and M. Torres, Phys. Rev. Lett. **80**, 1208 (1998).
[8] W. M. Robertson and J. F. Rudy III, J. Acoust. Soc. Am. **104**, 694 (1998).
[9] J. V. Sanchez-Pérez, D. Caballero, R. Martinez-Sala, J. Rubio, J. Sanchez-Dehesa, F. Meseguer, J. Llinares, and F. Galvez, Phys. Rev. Lett. **80**, 5325 (1998); D. Caballero, J. Sanchez-Dehesa, J. Rubio, R. Martinez-Sala, J. V. Sanchez-Perez, F. Meseguer, and J. Llinares, Phys. Rev. E **60**, R6316 (1999).
[10] M. Torres, F. R. Montero de Espinosa, D. Garcia Pablos, and N. Garcia, Phys. Rev. Lett. **82**, 3054 (1999).
[11] M. Torres, F. R. Montero de Espinosa, and J. L. Aragon, Phys. Rev. Lett. **86**, 4282 (2001).
[12] M. Kafesaki, M. M. Sigalas, and N. Garcia, Phys. Rev. Lett. **85**, 4044 (2000); Physica B **296**, 190 (2001).
[13] A. Khelif, B. Djafari-Rouhani, J. O. Vasseur, and P. A. Deymier, Phys. Rev. B **68**, 024302 (2003).

[14] I. E. Psarobas and M. M. Sigalas, Phys. Rev. B **66**, 052302 (2002).
[15] M. M. Sigalas and N. Garcia, J. Appl. Phys. **87**, 3122 (2000).
[16] Suxia Yang, J. H. Page, Zhengyou Liu, M. L. Cowan, C. T. Chan, and Ping Sheng, Phys. Rev. Lett. **88**, 104301 (2002).
[17] R. Sainidou, N. Stefanou, and A. Modinos, Phys. Rev. B **66**, 212301 (2002).
[18] I. E. Psarobas, N. Stefanou, and A. Modinos, Phys. Rev. B **62**, 278 (2000).
[19] Zhengyou Liu, Xixiang Zhang, Yiwei Mao, Y. Y. Zhu, Zhiyu Yang, C. T. Chan, and Ping Sheng, Science **289**, 1734 (2000).
[20] Zhengyou Liu, C. T. Chan, and Ping Sheng, Phys. Rev. B **65**, 165116 (2002).
[21] Zhengyou Liu, C. T. Chan, and Ping Sheng, A. L. Goertzen, and J. H. Page, Phys. Rev. B **62**, 2446 (2000).
[22] I. E. Psarobas, N. Stefanou, and A. Modinos, Phys. Rev. B **62**, 5536 (2000).
[23] A. Khelif, P. A. Deymier, B. Djafari-Rouhani, J. O. Vasseur, and L. Dobrzynski, J. Appl. Phys. **94**, 1308 (2003).
[24] See, for instance, Ph. Lambin, A. Khelif, J. O. Vasseur, L. Dobrzynski, and B. Djafari-Rouhani, Phys. Rev. E **63**, 066605 (2001), and references therein.
[25] Y. Tanaka and S. Tamura, Phys. Rev. B **58**, 7958 (1998); **60**, 13 294 (1999).
[26] A. Khelif, B. Djafari-Rouhani, J. O. Vasseur, P. A. Deymier, Ph. Lambin, and L. Dobrzynski, Phys. Rev. B **65**, 174308 (2002).
[27] A. Taflove, *The Finite Difference Time Domain Method* (Artech, Boston, 1998).
[28] C. T. Chan, Q. L. Yu, and K. M. Ho, Phys. Rev. B **62**, 7387 (2000).
[29] S. Fan, P. R. Villeneuve, and J. D. Joannopoulos, Phys. Rev. B **54**, 11 245 (1996).
[30] G. Mur, IEEE Trans. Electromagn. Compat. **23**, 377 (1981).
[31] M. Kafesaki, M. M. Sigalas, and E. N. Economou, Solid State Commun. **96**, 285 (1995).